

The role of collisions and strong coupling in ultracold plasmas

J Castro, P McQuillen, H Gao and T C Killian

Rice University, Department of Physics and Astronomy, 6100 Main St., Houston, Texas, USA 77005

E-mail: killian@rice.edu

Abstract. Ultracold plasmas are formed by photo-exciting clouds of cold atoms and molecules near the ionization threshold. They explore a new region of plasma physics and display effects of strong coupling, which is characterized by a ratio of Coulomb energy to kinetic energy that is greater than unity. Collisions of many types play a role in the creation, equilibration, and expansion of these systems.

1. Introduction

Ultracold neutral plasmas are formed by photo-exciting cold atoms and molecules near the ionization threshold, yielding electron temperatures from 1-1000K and ion temperatures around 1 K [1, 2]. At typical densities of $\sim 10^{10} \text{ cm}^{-3}$, the average Coulomb interaction energy between neighboring particles can be on the order of or exceed the thermal energy, which makes the plasma strongly coupled [3]. Strong coupling is relatively difficult to achieve experimentally, but it is important in many areas of physics. In ultracold plasmas it leads to spatial correlations, modification of thermalization timescales, and surprising equilibration dynamics. Ultracold plasmas also display many classic plasma phenomena such as various collective modes, Debye screening, and ambipolar diffusion.

Collisions of many types play prominent roles in the main stages of plasma evolution: formation, electron equilibration, ion equilibration, and plasma expansion (Fig. 1). When starting with a gas of highly excited Rydberg atoms, atom-atom and electron-atom collisions lead to ionization and plasma formation. Electron collisions, three-body recombination, and electron-Rydberg collisions dominate dynamics during electron equilibration. During the ion equilibration stage, ions heat due to interactions with neighboring ions, and collisional processes reflect strong coupling of the ions. During expansion, electrons and ions adiabatically cool, which eventually increases the three-body recombination rate. Formation of the plasma from molecules in a beam introduces predissociation, dissociative recombination, and collisions with neutral atoms forming the high pressure backing gas.

2. Strong Coupling

In strongly coupled plasmas, the Coulomb interaction energy exceeds the thermal energy, and this is parameterized by the Coulomb coupling constant

$$\Gamma = \frac{e^2}{4\pi\epsilon_0 a k_B T}, \quad (1)$$

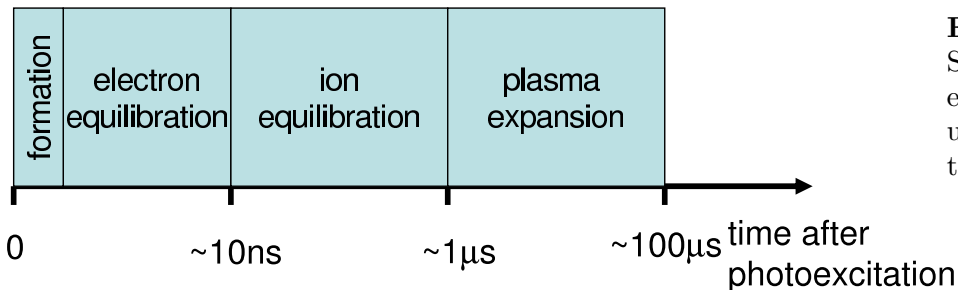


Figure 1. Stages in the evolution of an ultracold neutral plasma.

where T is the temperature and a is the Wigner-Seitz radius, $a = [3/(4\pi n)]^{1/3}$ for density n . Ions in ultracold neutral plasmas equilibrate with $2 < \Gamma_i < 5$ [4]. It is possible to set initial conditions that imply large electron Γ_e , but rapid heating processes involving many different collisional effects clamp the equilibrium $\Gamma_e \leq 0.2$ [5, 6, 7, 8].

Strong coupling is of interest in many areas of physics. In systems with $\Gamma > 1$, spatial correlations develop between particles, concepts such as Debye screening and hydrodynamics must be reexamined, and new phenomena appear, such as kinetic energy oscillations during equilibration [9]. Strongly-coupled plasmas appear in extreme environments, such as dense astrophysical systems [10], matter irradiated with intense-laser fields [11, 12], dusty plasmas of highly charged macroscopic particles [13], or non-neutral trapped ion plasmas [14] that are laser-cooled until they freeze into a Wigner crystal. Ultracold neutral plasmas offer unique opportunities for studying strong coupling, especially because the method of forming the plasma allows equilibration processes to be studied in great detail.

3. Creation of an Ultracold Neutral Plasma

3.1. Direct Photoionization of Laser-Cooled Atoms

The most common method for creating an ultracold neutral plasma is to start with laser-cooled and trapped neutral atoms in a magneto-optical trap (MOT)[15]. Most experiments use alkali metal atoms, alkaline-earth metal atoms, or metastable noble gas atoms because their principal transitions are at convenient laser wavelengths. Depending upon the element chosen, up to 10^{10} atoms can be trapped, and the density can be as high as 10^{12} cm^{-3} , but most experiments are conducted with about 100 times lower values. The temperature is in the microkelvin to millikelvin range. The density distribution is typically a spherical Gaussian, with a characteristic radius of about 1 mm, which also determines the density profile of the plasma.

The plasma is created through single or multi-photon processes usually involving a 10 ns pulsed dye laser whose wavelength is tuned just above the ionization continuum, and the ionization fraction can approach 75%. Because of the small electron-ion mass ratio, the electrons have an initial kinetic energy approximately equal to the difference between the photon energy and the ionization potential, typically between 1 and 1000 K. The initial kinetic energy for the ions is close to the kinetic energy of neutral atoms in the MOT.

3.2. Plasma Creation from Rydberg Atoms

If the ionizing laser wavelength is tuned just below the ionization threshold, a dense gas of highly excited Rydberg atoms is created. It was noted very early in the study of these systems that in a low electric field environment, in which free electrons are not quickly removed from the system, electron-atom collisions can drive a spontaneous ionization cascade [16, 17]. Approximately two-thirds of the atoms are ionized, and the remaining fraction are driven to more deeply bound

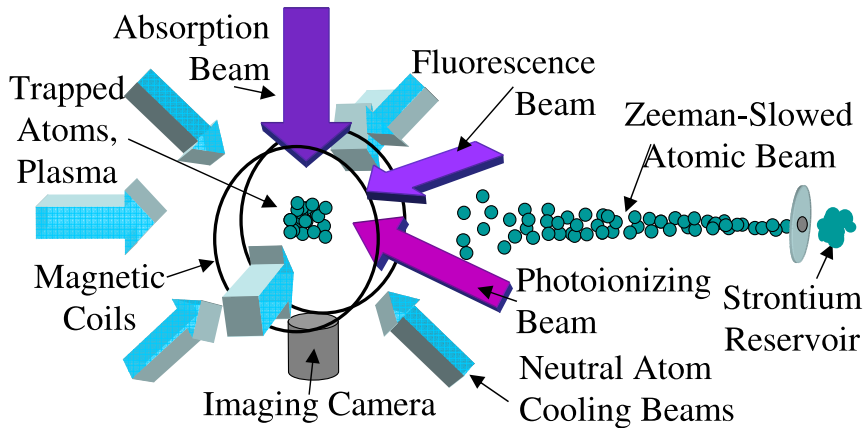


Figure 2. Typical experimental schematic for creating an ultracold plasma from laser cooled atoms in a MOT [4]. The MOT for neutral atoms consists of a pair of anti-Helmholtz magnetic coils and 6 laser-cooling beams. Atoms from a Zeeman-slowed atomic beam enter the MOT region, are trapped, and then ionized by the photoionizing laser. Optical imaging diagnostics, such as absorption and fluorescence imaging, can be used for alkaline-earth metal plasmas. For charged particle detection diagnostics, electron or ion multipliers and electric field-generating wires or meshes are added to the vacuum system to detect charges that escape from the plasma.

states, satisfying conservation of energy.

This formation process is quite complex. Initial electrons are produced by blackbody ionization [17] or ionizing collisions of initially stationary atoms that are driven by resonant dipole-dipole attractive interactions [18]. Electrons also efficiently drive angular momentum-changing collisions and rapidly mix the ℓ values of the Rydberg atoms [19].

It is interesting to note that independent of the creation technique, during the expansion of ultracold plasmas, a significant fraction ($\geq 10\%$) of the charges recombine to form Rydberg atoms [20], presumably through three-body recombination [21, 8].

3.3. Plasma Creation from Molecular Beams

A recent advance in the field, which greatly expands the types of plasmas that can be formed and the collisional processes present is the creation of an ultracold plasma in a supersonic molecular beam [22]. The effective translational temperature in the moving frame of reference of atoms or molecules seeded in the expansion of a high pressure (≥ 1 atm), typically inert, backing gas can be in the range of 1 K. Rotational and vibrational temperatures can also be reduced. Such beams have been valuable tools in chemistry and physics for many years (e.g.[23]) because of the utility of the cold samples for experiments and general applicability to any atomic and molecular species.

A supersonic beam is an attractive starting point for forming an ultracold plasma because the density of target species can be high ($\geq 10^{12}$ cm $^{-3}$), photoexcitation of a well defined volume of gas is easily accomplished with pulsed lasers, and it gives easy access to cold molecules, which are currently challenging to produce in any other way at high density. Morrison *et al.* [22] excited a dense gas of NO Rydberg molecules in this way and observed the spontaneous evolution into a plasma, exactly as observed in [16, 17]. A time-of-flight charged particle diagnostic was used to demonstrate that a stable, quasi-neutral plasma was formed. The rate of plasma expansion was used to infer that the plasma was ultracold, as expected, with an electron temperature as low as 7 K [24]. This experiment raises many exciting possibilities, such as further cooling of ions in

the plasma through collisions with the background gas and the introduction of new collisional phenomena, such as predissociation and dissociative recombination, which may affect plasma dynamics.

4. Diagnostics

A full description of UNP diagnostic techniques can be found in [2]. Charged particle detection of ions or electrons is the most common technique because of its simplicity and applicability to any type of plasma. Information can be extracted on the rate of escape of electrons from the plasma [25], the spatial distribution of ions [22], and the response of the plasma to external perturbation [26], such as a radio-frequency field. In conjunction with pulsed-field ionization, charged particle diagnostics can be used to measure Rydberg atom populations in the plasma [19, 18]. Optical imaging techniques, which use lasers resonant with a principal transition in the ions, have proven very powerful because they can measure the ion kinetic energy and temperature [9, 27]. But they have only been used with plasmas formed from alkaline-earth metal atoms, which have ions with principal transitions in the visible. Fluorescence imaging has recently been used to separate the large ion kinetic energy due to plasma expansion from thermal kinetic energy [28].

5. Electron Equilibration

When the plasma is formed, both electrons and ions are far from equilibrium, and most ultracold neutral plasma studies have focused on the establishment of local and global thermal equilibrium. This topic takes on particular interest because the plasma is in or near the strongly coupled regime. For a thorough review, see [2].

5.1. Disorder-Induced Heating

As the name suggests, disorder-induced heating (DIH) stems from the fact that immediately after plasma creation, charged particles are spatially uncorrelated, which yields greater potential energy than the equilibrium state. On a timescale of the inverse electron plasma frequency, $\omega_{pe}^{-1} = \sqrt{m_e \epsilon_0 / n_e e^2}$, where m_e is the electron mass and e is the electron charge, which is on the order of a few nanoseconds, short range correlations develop between electrons and ions and electrons and electrons. This decreases the potential energy and increases the kinetic energy by about $e^2 / (4\pi\epsilon_0 a)$ per particle, which heats electrons typically by a few degrees kelvin [8]. Kuzmin et al. [29] showed that correlations develop until the Coulomb coupling parameter approaches $\Gamma_e \sim 1$.

5.2. Coulomb Collisions

During DIH, the electron velocity distribution is also thermalizing due to Coulomb collisions. The timescale for this process is given by the Spitzer-Landau formula [30],

$$\tau_{ee} \sim \frac{2\pi\epsilon_0^2 m_e^{1/2} (3k_B T_e)^{3/2}}{n_e e^4 \ln(\Lambda_e)}, \quad (2)$$

where $\ln(\Lambda_e) = \ln(4\pi\epsilon_0 3k_B T_e \lambda_{D,e} / e^2)$ is the so-called Coulomb logarithm for the electrons with $\lambda_{D,e} = \sqrt{\epsilon_0 k_B T_e / (n_e e^2)}$ as the electron Debye screening length. For $T_e = 40$ K and $n_e = 10^{15} \text{ m}^{-3}$, $\tau_{ee} \sim 10$ ns. After thermalization, they can be described with a Maxwell-Boltzmann distribution and a well-defined local temperature [5, 31].

The mean-free-path for electrons is longer than the plasma size, so the electrons are in good thermal contact with each other. Nonetheless there can be small variations in electron temperature due to the spatial dependence of the potential seen by electrons and the fact that electrons escape from the edge of the plasma [5]. Many papers have studied various aspects of the electron dynamics [21, 5, 6, 7, 8] such as ambipolar diffusion and trapping of electrons in the potential formed by the ions [25].

5.3. Three-Body Recombination

Three-body recombination (TBR) [32] refers to the process in which an ion and electron recombine to form highly excited Rydberg atoms and the energy released in this process is taken up by a second electron to conserve energy and momentum. The rate of TBR, per ion [32, 6], is given as

$$R = 3.9 \times 10^{-21} \text{s}^{-1} \left[n_e (\text{m}^{-3}) \right]^2 [T_e (\text{K})]^{-9/2}. \quad (3)$$

As the TBR rate varies with electron temperature as $T_e^{-9/2}$, this is the dominant recombination mechanism in UNPs [20]. Because TBR acts as a heating mechanism for the electrons and the rate increases so rapidly with decreasing temperature, TBR acts as a natural feedback mechanism, which has been shown experimentally and theoretically to keep the $\Gamma_e \leq 0.2$ [5, 6, 7, 8].

There has been much debate about the validity of the TBR expression, Eq. 3, for ultracold plasmas in which the electron temperatures are very low, e.g. [33, 7, 29, 5, 26]. A recent Monte Carlo calculation appropriate to conditions in an UNP [34] found slight deviations from the classic expressions [32] at very low collision energies, which decreases the overall rate by 30% but does not qualitatively change the behavior. This discussion is complicated by the challenge of describing rates in a system that is, strictly speaking, not in equilibrium. Also, electrons and ions are constantly forming weakly bound states that are quickly disrupted by plasma microfields, so even the definition of a Rydberg atom can be called into question. But a convergence seems to be emerging around theory [34] and experimental results measuring the rate at which Rydberg states are repopulated after being emptied by an RF pulse [26].

5.4. Rydberg-electron collisions

A collision between a Rydberg atom and an electron in the plasma tends to ionize the Rydberg atom if it is bound by less than about $4k_B T$ and drive it to lower energies if it is bound by more than this. This leads to a “kinetic bottleneck” in the population [34], but it also leads to significant further heating of the plasma electrons [5, 8] since a tremendous amount of energy can be released during de-excitation. It has also been shown that electron-Rydberg collisions in UNPs are extremely efficient at randomizing the distribution of occupied electron orbital angular momentum states [19].

6. Ion Equilibration

The ions in strontium UNPs are created with kinetic energies reflecting the millikelvin or microkelvin temperature of atoms in the MOT. This would suggest very large Γ_i and very strong spatial correlations. But immediately after plasma formation, the ions are far from thermal equilibrium, and the equilibration process drastically changes the kinetic energy distribution and displays phenomena that reflect strong coupling.

6.1. Disorder-Induced Heating

DIH affects the ions just as it does the electrons. It raises the ion temperature to about 1 K (Fig. 3) and acts as a feedback mechanism to always produce $2 < \Gamma_i < 5$ [4, 9]. The timescale, given by the inverse ion plasma oscillation frequency $\omega_{pi}^{-1} = \sqrt{m_i \epsilon_0 / n_i e^2} \sim 1 \mu\text{s}$, where, n_i is the ion-density and m_i is the mass of the ion, is much slower than for electrons. Debye screening by the electrons modifies the equilibrium ion temperature, and this effect is well described by modelling the ion-ion interaction as a Yukawa interaction [35] even when there are only a few electrons per Debye sphere [9].

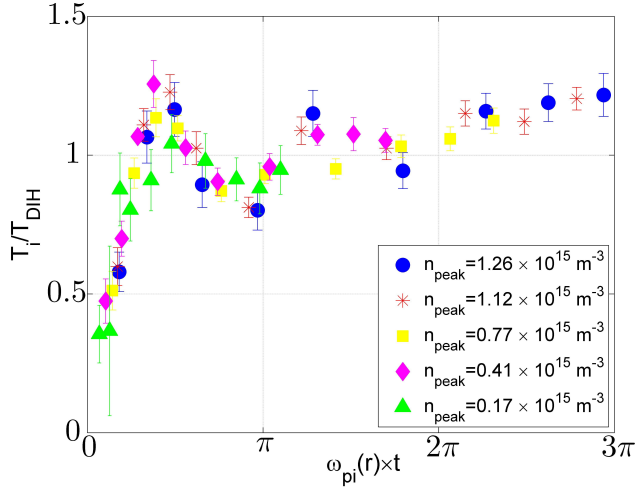


Figure 3. Disorder-induced heating and kinetic energy oscillations in a UNP. As spatial correlations develop, ion potential energy is converted to kinetic energy to a value given by $T_{DIH} \sim 1$ K [35]. The kinetic energy will oscillate about its equilibrium value with the plasma frequency, $\omega_{pi} \propto n^{1/2}$. The figure shows how disorder-induced heating and the oscillation frequency scale for UNPs with different densities.

6.2. Kinetic Energy Oscillations

During equilibration, strong coupling gives rise to oscillations in the kinetic energy at $2\omega_{pi}$ reflecting each ion's oscillation at frequency ω_{pi} in the potential well formed by the cage of nearest neighbors. Approximately one coherent oscillation is observable, before collisional processes and nonuniformity of the potential wells seen by each ion, damp the oscillation. DIH can be viewed as the beginning of this oscillation. This phenomenon was first observed experimentally in [9] and modeled more extensively in [36, 37], and similar dynamics should occur in plasmas produced by intense radiation of solid and foil targets [37]. Although there is no long-range spatial coherence in the oscillation, it is instructive to think of this motion as an ion plasma oscillation, which is the short wavelength limit of the ion electrostatic wave. Figure 3 shows kinetic energy oscillations for UNPs with different densities and its scaling with density.

6.3. Coulomb Collisions

Traditionally, the equilibration time scale for the ion velocity distribution is calculated with the Spitzer-Landau formula [30],

$$\tau_{ii} \sim \frac{2\pi\epsilon_0^2 m_i^{1/2} (3k_B T_i)^{3/2}}{n_i e^4 \ln(\Lambda_i)}, \quad (4)$$

where, for the ions and for $T_i \ll T_e$, the Coulomb logarithm is now evaluated as $\ln(\Lambda_i) = \ln(4\pi\epsilon_0 3k_B T_i \lambda_{D,i} / e^2)$ with the ion Debye screening length of $\lambda_{D,i} = \sqrt{\epsilon_0 k_B T_i / (n_i e^2)}$. In terms of the coupling parameter Γ , the logarithm may be written as $\ln(\Lambda_i) = \ln(\sqrt{3}/\Gamma_i^{3/2})$. This expression diverges when the temperature and density correspond to a strongly coupled plasma, $\Gamma_i > 1$.

To understand this the origin of this divergence, note that the Spitzer-Landau time is calculated from the energy exchange time in a collision between charged particles [30]. This calculation involves the velocity diffusion coefficients found by integrating over all possible impact parameters, ρ . This integration diverges due to contributions of large impact parameters. Canonically, this divergence is removed by introducing an upper limit cut-off at $\rho_{max} = \lambda_{D,i}$, the ion Debye screening length. This is a physically sensible cutoff in weakly coupled plasmas in which there are many particles within a sphere of radius λ_D . But in strongly coupled systems, as the Debye screening length becomes similar to the interparticle spacing, it is no longer suitable as the upper limit cut-off, and the Spitzer formula becomes invalid.

Many alternative cutoffs and expressions for τ_{ii} have been proposed to remove the divergence of the Coulomb logarithm in strongly coupled systems [38]. This is an important problem since Coulomb collisions and associated relaxation times are crucial to inertial confinement fusion experiments [39]. UNPs can thus provide a good tool to study this problem.

6.4. Collisions with Background Neutral Atoms

Collisions between ions and neutral atoms and molecules at ultracold temperatures [40] have attracted increased attention recently, in part because of experiments creating overlapping trapped atoms and ions [41]. Ultracold plasmas formed by photoexciting molecules seeded in a supersonic beam [22] provide a new opportunity to study such phenomena, and the collisions may serve a valuable function by removing disorder-induced heat from the ions to produce much stronger coupling. Large elastic collision cross-sections, $\sigma \sim 10^{-10} \text{ cm}^2$ [40], at collision energies near 1 K lead to collision times below 1 ms for a background gas density $\sim 10^{12} \text{ cm}^{-3}$.

7. Conclusion

With the introduction of new diagnostics, such as fluorescence imaging, and new techniques, such as formation of plasmas in supersonic beams, the range of phenomena accessible for study in UNPs continues to expand. Collisions of many types are central to the dynamics of these system, and strong coupling adds interesting new features to familiar processes such as equilibration.

Acknowledgments

This work is supported by the U.S. National Science Foundation-DOE Partnership and the David and Lucille Packard Foundation. J.C. thanks MICIT and CONICIT of Costa Rica for financial support.

- [1] Killian T C 2007 *Science* **316** 705
- [2] Killian T C, Pattard T, Pohl T and Rost J M 2007 *Phys. Rep.* **449** 77
- [3] Ichimuru S 1982 *Rev. Mod. Phys.* **54** 1017
- [4] Simien C E, Chen Y C, Gupta P, Laha S, Martinez Y N, Mickelson P G, Nagel S B and Killian T C 2004 *Phys. Rev. Lett.* **92** 143001
- [5] Robicheaux F and Hanson J D 2003 *Phys. Plasmas* **10** 2217
- [6] Kuzmin S G and O'Neil T M 2002 *Phys. Plasmas* **9** 3743
- [7] Mazevet S, Collins L A and Kress J D 2002 *Phys. Rev. Lett.* **88** 55001
- [8] Gupta P, Laha S, Simien C E, Gao H, Castro J, Killian T C and Pohl T 2007 *Phys. Rev. Lett.* **99** 75005
- [9] Chen Y C, Simien C E, Laha S, Gupta P, Martinez Y N, Mickelson P G, Nagel S B and Killian T C 2004 *Phys. Rev. Lett.* **93** 265003
- [10] Horn H M V 1991 *Science* **252** 384
- [11] Nantel M, Ma G, Gu S, Cote C Y, Itatani J and Umstadter D 1998 *Phys. Rev. Lett.* **80** 4442
- [12] Springate E, Hay N, Tisch J W G, Mason M B, Ditmire T, Hutchinson M H R and Marangos J P 2000 *Phys. Rev. A* **61** 063201
- [13] Morfill G E, Thomas H M, Konopka U and Zuzic M 1999 *Phys. Plasmas* **6** 1769
- [14] Mitchell T B, Bollinger J J, Huang X P, Itano W M and Dubin D H E 1999 *Phys. Plasmas* **6** 1751
- [15] Metcalf H J and van der Straten P 1999 *Laser Cooling and Trapping* (New York: Springer-Verlag)
- [16] Rolston S L, Bergeson S D, Kulin S and Orzel C 1984 *Bull. Am. Phys. Soc.* **43** 1324
- [17] Robinson M P, Tolra B L, Noel M W, Gallagher T F and Pillet P 2000 *Phys. Rev. Lett.* **85** 4466
- [18] Li W, Tanner P J and Gallagher T F 2005 *Phys. Rev. Lett.* **94** 173001
- [19] Dutta S K, Feldbaum D, Walz-Flannigan A, Guest J R and Raithel G 2001 *Phys. Rev. Lett.* **86** 3993
- [20] Killian T C, Lim M J, Kulin S, Dumke R, Bergeson S D and Rolston S L 2001 *Phys. Rev. Lett.* **86** 3759
- [21] Robicheaux F and Hanson J D 2002 *Phys. Rev. Lett.* **88** 55002
- [22] Morrison J P, Rennick C J, Keller J S and Grant E R 2008 *Physical Review Letters* **101** 205005
- [23] Gordon R J, Lee Y T and Herschbach D R 1971 *The Journal of Chemical Physics* **54** 2393
- [24] Morrison J P, Rennick C J and Grant E R 2009 *Physical Review A (Atomic, Molecular, and Optical Physics)* **79** 062706
- [25] Killian T C, Kulin S, Bergeson S D, Orozco L A, Orzel C and Rolston S L 1999 *Phys. Rev. Lett.* **83** 4776
- [26] Fletcher R S, Zhang X L and Rolston S L 2007 *Physical Review Letters* **99** 145001

- [27] Cummings E A, Daily J E, Durfee D S and Bergeson S D 2005 *Phys. Rev. Lett.* **95** 235001
- [28] Castro J, Gao H and Killian T C 2008 *Plasma Phys. Control. Fusion* **50** 124011
- [29] Kuzmin S G and O'Neil T M 2002 *Phys. Rev. Lett.* **88** 65003
- [30] Spitzer, Jr L 1962 *Physics of Fully Ionized Gases* (Wiley, New York)
- [31] Pohl T, Pattard T and Rost J M 2004 *Phys. Rev. A* **70** 033416
- [32] Mansbach P and Keck J 1969 *Phys. Rev.* **181** 275
- [33] Hahn Y 1997 *Phys. Lett. A* **231** 82
- [34] Pohl T, Vrinceanu D and Sadeghpour H R 2008 *Phys. Rev. Lett.* **100** 223201
- [35] Murillo M S 2001 *Phys. Rev. Lett.* **87** 115003
- [36] Laha S, Chen Y C, Gupta P, Simien C E, Martinez Y N, Mickelson P G, Nagel S B and Killian T C 2006 *Euro. Phys. J. D* **40** 51
- [37] Murillo M S 2006 *Phys. Rev. Lett.* **96** 165001
- [38] Gericke D O, Murillo M S and Schlanges M 2002 *Phys. Rev. E* **65** 036418
- [39] Glosli J N, Graziani F R, More R M, Murillo M S, Streitz F H, Surh M P, Benedict L X, Hau-Riege S, Langdon A B and London R A 2008 *Physical Review E* **78**
- [40] Côté R and Dalgarno A 2000 *Phys. Rev. A* **62** 012709
- [41] Grier A T, Cetina M, Oručević F and Vuletić V 2009 *Physical Review Letters* **102** 223201